Vol. 3 No. 2, Dec. 2023

FUAM Journal of Pure and Applied Science

Available online at
www.fuamjpas.org.ng

An official Publication of
College of Science
Joseph Sarwuan Tarka University,
Makurdi.

FUAM Journal of Pure and Applied Science
© College of Science, Joseph Sarwuan Tarka University, Makurdi
https://fuamjpas.org.ng/
Vol.3. No. 2. December, 2023

Structural Analysis of Pure and Magnesium Doped Barium Titanate Ceramic

F.M. Lariski* and H. Abdulsalam
Department of Physics, Faculty of Science, Yobe State University, Damaturu, Yobe State, Nigeria.
*Correspondence E-mail: fmusalariski@gmail.com

Received: 18/08/2023 **Accepted**: 26/10/2023 **Published online**: 19/11/2023

Abstract
This research focuses on the synthesis and analysis of barium titanate samples, both pure and magnesium-doped, using the sol-gel auto combustion method. The samples were categorized into three groups with the chemical formula $Ba_{1-x}Mg_xTiO_3$, where x takes values of 0.00, 0.10, and 0.20. Through X-ray diffraction patterns, the formation of a perovskite structure with a singular phase was confirmed in all samples. Notably, the pure barium titanate sample exhibited a prominent absorption peak at 495 cm^{-1}, while the doped composites with x values of 0.10 and 0.20 displayed absorbance peaks at 497 cm^{-1} and 499 cm^{-1}, respectively. The use of Fourier Transform Infrared spectroscopy and Field Emission Scanning Electron Microscopy corroborated the presence of polycrystalline microstructures, characterized by a measurable degree of porosity that aligns well with X-ray diffraction analysis. Particle distribution demonstrated a normal distribution pattern. Energy Dispersive Spectroscopy further confirmed the elemental composition, revealing the presence of Ba, Ti, and O, as well as minimal traces of Mg impurities. This study underscores the successful synthesis and characterization of $Ba_{1-x}Mg_xTiO_3$ samples, contributing to the understanding of their structural and compositional properties.

Keywords: Barium titanate, Ceramic, Magnesium, Structural. XRD,

Introduction

Barium titanate ($BaTiO_3$) is a classic example of a ferroelectric material, characterized by its perovskite-type structure. There is a substantial focus on researching the potential applications of $BaTiO_3$, in microwave devices, Dynamic Random-Access Memory (DRAM), and the Multi-Layer Ceramic Capacitors (MLCC). This is attributed to its significant dielectric properties, minimal leakage current, and impressive breakdown electric field. In the case of $BaTiO_3$, doping-induced core-rim arrangement has the potential to change the temperature at which a phase transition takes place and to smoothen out the temperature dependency of the capacitance curve [1][2]. Above its curie temperature, Tc (130 °C), the crystal structure's symmetry has been found to be Pseudo-cubic [3]. Dielectric materials must have high permittivity values at room temperature and be electrically insulating in order to be used in MLCCs. Devices for overload protection must be semiconductors at ambient temperature and have a rapid increase in resistance at the Curie temperature. [4]. Due to its superior dielectric, piezoelectric, and ferroelectric properties, $BaTiO_3$ is the most widely used ferroelectric material and is utilized in capacitors, ferroelectric memories, and other applications. [5]. Temperature, as well as the frequency and rate of a time-varying electric field, have a significant impact on dielectric parameters, including the dielectric constant and dielectric loss (tan δ). A wide range of frequencies shows these characteristics. [6]. Strain, charge, charge distribution, and ionic size all affect the substitutional chemistry when the dopants are integrated into the BT lattice. [7]. By using the traditional solid-state reaction approach, pure and Mg-doped barium titanate ceramics were created. Investigation was conducted into the crystal structure, surface morphology, and dielectric properties of ceramics comprising barium titanate doped with magnesium (Mg). When the concentration of Mg remains below 5 at-%, $Mg2^+$ ions are successfully incorporated into the unit cell. This incorporation preserves the perovskite structure within the solid solution, with no observable evidence of additional phases. However at Mg concentrations exceeding 5 at-%, a secondary phase of MgO becomes evident. Interestingly, it was observed that the presence of Mg can effectively impede the grain growth in barium titanate ceramics. These findings, as outlined by Cai et al., shed light on the role of Mg doping in influencing the material's structural and morphological attributes [5]. Materials like BaZrO3, BaSnO3, $MgTiO_3$, and $SrTiO_3$ can be produced by replacing isovalent cations, Zr^{4+}, Sn^{4+} for Ti^{4+} and/or Mg^{2+}, Sr^{2+} for Ba^{2+}, with Zr^{4+}, Sn^{4+}, or both. These combine with $BaTiO_3$ to generate solid solutions, which change the lattice constant, shift the phase transition temperature, and result in a high and broad maximum dielectric constant. [8]. $BaTiO_3$ is constituted of perovskite-based metal oxide minerals that can form cubic and tetragonal crystals structures at room temperature, which are the most researched structures. [9]. However, under ambient conditions, the tetragonal form exhibits the most stable structure. $BaTiO_3$-based materials offer a wide range of possible uses; however, due to their limited range of tetragonal stability and lower piezoelectric coefficient, they have encountered several practical restrictions. The current research strategy is motivated by the possibility of synthesizing new systems by substituting other ions of equivalent ionic sizes for Ba^{2+} or Ti^{4+} in order to further enhance the ferroelectric and dielectric properties of $BaTiO_3$. In fact, the perovskite structures exhibit considerable flexibility and an inherent ability to host ions of various sizes, and perovskite-based metal oxide materials can integrate a wide variety of different dopants at the Ba sites or the Ti sites. [9]. The sol-gel process involves

solidifying a compound with a highly chemically active component through a solution, sol, or gel, and then heating an oxide or other compound to make the material under mild conditions. [10]. Compared to other approaches now in use, it is more popular and has industrial applications. [11]. In this paper we study, the role of an individual magnesium dopant, on the structure of barium titanate-based ceramics. This material can be represented by the following formula, $Ba_{1-x}Mg_xTiO_3$ (x = 0.0, 0.1, 0.2). The tolerance factor of magnesium-doped barium titanate ceramic was calculated by using equation 1.

$$t = \frac{(r_A + r_O)}{\sqrt{2}(r_B + r_O)} \qquad 1$$

The t value also provides an indication about how far the atoms can move from the ideal packing positions and be still "tolerated" in the perovskite structure. [12]. where t is the tolerance factor. r_A , r_B and r_O represent the ionic radii of the A site cation, the B site cation and the oxygen anion respectively. Stable perovskites usually satisfy 0.78 < t ≤ 1.05. It is a perfect perovskite structure when t = 1. The structure type would change if the t value is greater than this range. [13].

Materials and Methods

Chemicals and reagents

All chemical reagents used were of high quality (Analytical grade). The chemicals include, Barium nitrate [Ba $(NO_3)_2$] (Loba Chemie) Titanium dioxide (TiO_2) (Loba Chemie) magnesium nitrate [Mg $(NO_3)_2$], (Loba Chemie) Citric acid ($C_6H_8O_7$) (Loba Chemie) with distilled water as the solvent. The Stochiometric amount (grams) of chemical is given in Table 1. All the chemicals and reagents were used as received without any further purification.

Table 1 Stochiometric Amount of Chemical Used in $Ba_{1-x}Mg_xTiO_3$ Synthesis.

S/No.	x	Ba (grams)	Ti (grams)	Citric acid (grams)	Mg (grams)	Code
1.	0.00	13.066	3.995	38.426	Nil	T1
2.	0.10	11.759	3.995	38.426	0.7415	T2
3.	0.20	10.453	3.995	38.426	1.483	T3

Experimental detail

Mg^{2+} substituted $BaTiO_3$ with chemical composition $Ba_{1-x}Mg_xTiO_3$ (x = 0.0, 0.1, 0.2) have been successfully synthesized using sol-gel technique. Appropriate amount of the chemicals was dissolved in 100ml of distilled water in stoichiometric ratios to form an aqueous solution. The molar ratio of citric acid to cation was maintained at 1:2. The prepared solution was heated at a temperature of 80–100°C. The solution was stirred using constant and continuous magnetic stirrer in order to evaporate the water; a white gel was obtained which was transferred to a hot plate and heated at a temperature of 280–300 °C. This gives a black precursor material which was grounded with mortar and pestle to obtain a fine barium titanate precursor which was pre calcinated in a digital controlled muffle furnace at 900°C for 5 h. The pre-calcinated powder was divided into three parts and labeled T1, T2, and T3. Furthermore, T1, T2 and T3 were further heated at 1100°C for 5 h. The obtained product was crushed using mortar and pestle to obtain the fine barium titanate ceramic powder followed by various characterizations.

Characterization tools

Structural and phase analysis were carried out with a Bruker AXS D8 advanced X-ray diffraction analysis (XRD) diffractometer. Functional groups were also evaluated from Fourier Transform Infrared Spectroscopy (FTIR) spectra obtained with Nicolet FTIR interferometer IR prestige-21(model 8400S). The morphology and elemental analysis were studied using Field Emission Scanning Electron Microscopy (FE-SEM) (FEI Nova NanoSEM 450 FE-SEM).

Results and Discussion

XRD analysis

The XRD patterns of $Ba_{1-x}Cu_xTiO_3$ (x = 0.0, 0.1, and 0.15) are shown in Figure 1. The diffraction peaks observed were indexed using JCPDS card number 79-2263.[14].

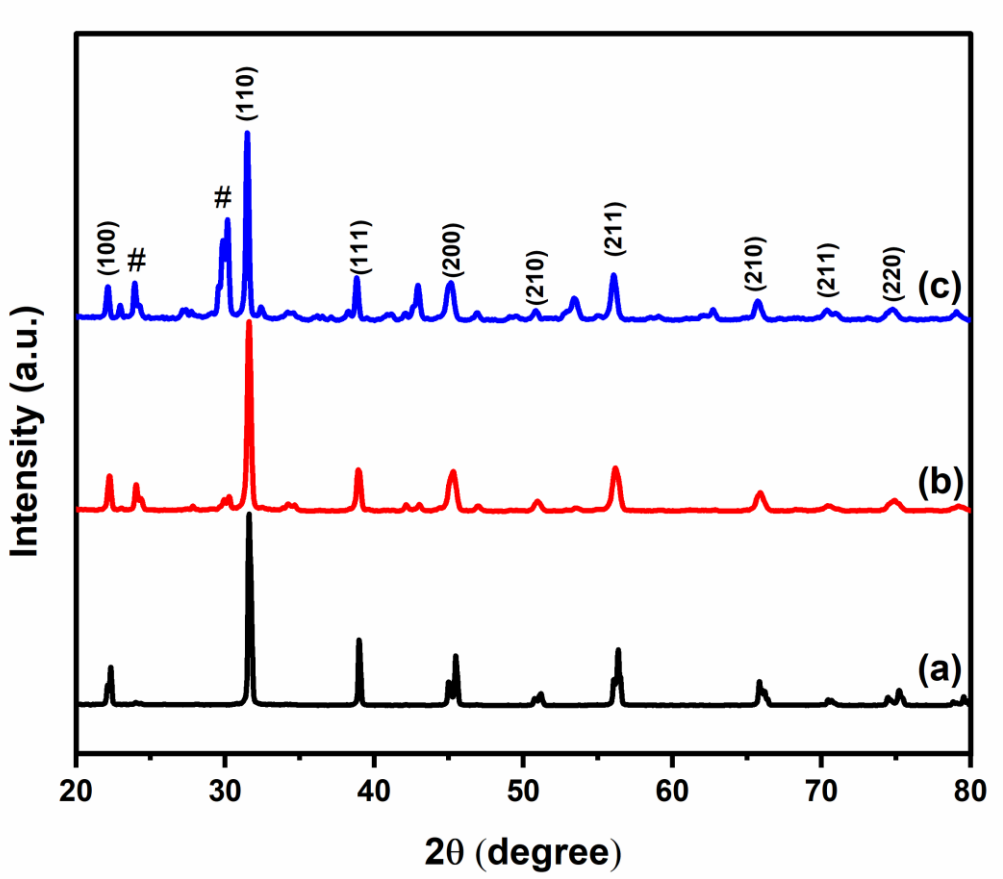

Fig 1: XRD patterns of $Ba_{1-x}Mg_xTiO_3$ (x = 0.00, 0.10, and 0.20).

The existence of the (100), (110), (111), (200), (210) and (211) major lattice planes in the XRD patterns confirms the formation of perovskite structure. The tolerance factor (t) of this composition $Ba_{1-x}Mg_xTiO_3$ is 0.947 and this also confirms a cubic structure for the sample. the other impurity phases are obtained during synthesis. In all the samples, the impurity phase was observed and it was shown as # in Fig. 1 and it may be attributed to $BaMgTiO_3$. From the XRD pattern, a shift was observed in the (200), (211) and (220), this shift indicates that the lattice constant of Mg doped BTO ceramics decreases with increasing the MgO content. It can be explained that Mg^{2+} ions substitute for Ba^{2+} ions on the A sites of the barium titanate lattice. It has been discovered that the difference between the ionic radii of the Ba (1.35A°) and Mg (0.72A°) as a result, the lattice constant and the cell volume decrease when lower radii of Mg are substituted for larger radii of Ba. The lattice constant (a) and the volume of the unit cell (V_{cell}) were calculated using Equations 2 and 3.

$$a = d\sqrt{h^2 + k^2 + l^2} \qquad 2$$

$$V_{cell} = a^3 \qquad 3$$

Where *d* is the interplanar spacing, *h, k* and *l* are the Miller indices. (h, k, l) = (100) the lattice constant, the interplanar spacing and the volume of the unit cell are shown in the Table 1.

Table 2 Lattice constant, Interplanar spacing and Volume of the unit cell

x	**0.00**	**0.10**	**0.20**
d (Å)	4.0065	3.9951	3.9940
a (Å)	4.0065	3.9951	3.9940
V_{cell} (Å^3)	64.3125	63.7650	63.7124

FTIR analysis

Figure 2 shows the FTIR spectra of $Ba_{1-x}Mg_xTiO_3$ (x = 0.00, 0.10, and 0.20) in the wave number range 400-4000 cm^{-1}. To examine the impact of additives and identify the local symmetry in the ceramics, the FTIR techniques were used. [15]. For the pure barium titanate powder, a powerful absorption peak is obtained at 512cm^{-1}, for the doped compositions for x = 0.10 and x = 0.20, absorbance peaks are obtained at 493cm^{-1} and 499cm^{-1} appropriately and 1440cm^{-1}. FTIR research confirmed that the ceramic nanoparticles formed a perovskite structure as seen in, [16].

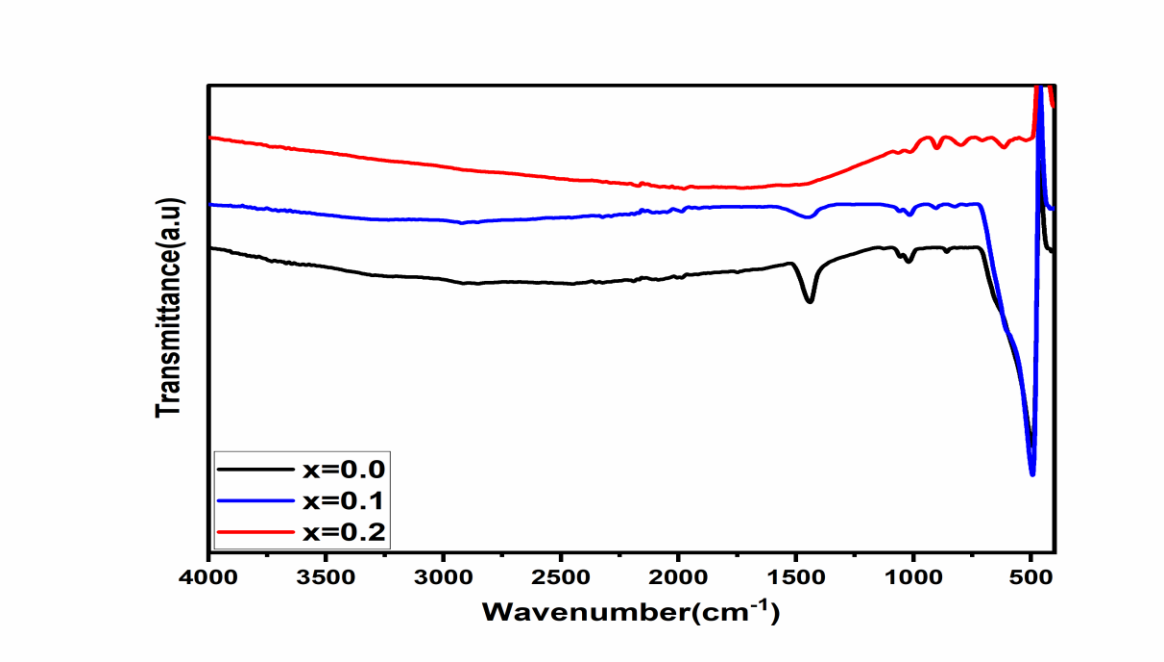

Fig 1: FTIR spectra of $Ba_{1-x}Mg_xTiO_3$ (x = 0.00, 0.10, and 0.20).

FE-SEM Analysis

FE-SEM and EDS were used to analyze the material's surface morphology. [17]. Figure 3 (a) and (c) show the field emission scanning electron microscopy micrographs of the sample $Ba_{1-x}Mg_xTiO_3$ (x = 0.00, and 0.20), prepared at 1,100 ◦C for 5 h. micrographs confirm the presence of the polycrystalline microstructure with certain degree of porosity in good agreement with XRD results. Fig. 3 (b) and (d) show that the particles follow a normal distribution, with average particle sizes of 44nm and 45nm for x = 0.00 and x = 0.20 respectively, that is to say the particle size increases with Mg^{2+} concentrations.

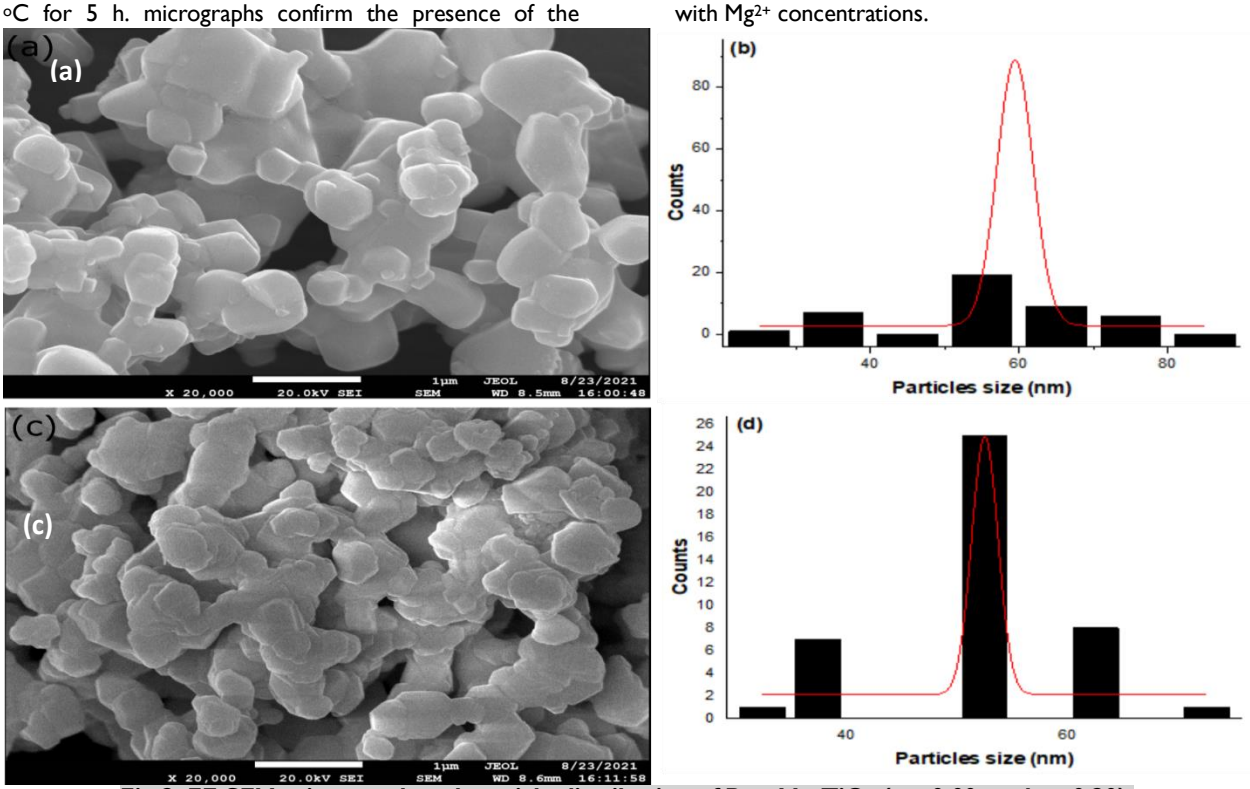

Fig 2: FE-SEM micrograph and particle distribution of $Ba_{1-x}Mg_xTiO_3$ (x = 0.00, and x= 0.20).

The result indicates that Mg can inhibit grain growth of BTO ceramics. This is because that Mg^{2+} ions dissolve into barium titanate lattice to substitute for Ba^{2+} ions on the A sites and oxygen vacancies are simultaneously generated, the appearance of oxygen vacancy can lead to lattice distortion and lattice distortion shall consume some energy, but if appearance of solute segregation will not consume the energy, Mg^{2+} ions are prone to segregate on the grain boundary. Mg^{2+} ions located in the grain boundary baffle motion of the grain boundary and accordingly inhibited grain growth of the BTO ceramics.

The Energy Dispersive X-ray (EDX) spectra Figure 4 (a) taken at a number of randomly selected positions of the sample shows the expected presence of Ba, Ti, and O. Figure 4 (b) also confirms the formation of Ba, Ti, and O, with some impurity of Mg present in negligible amount.

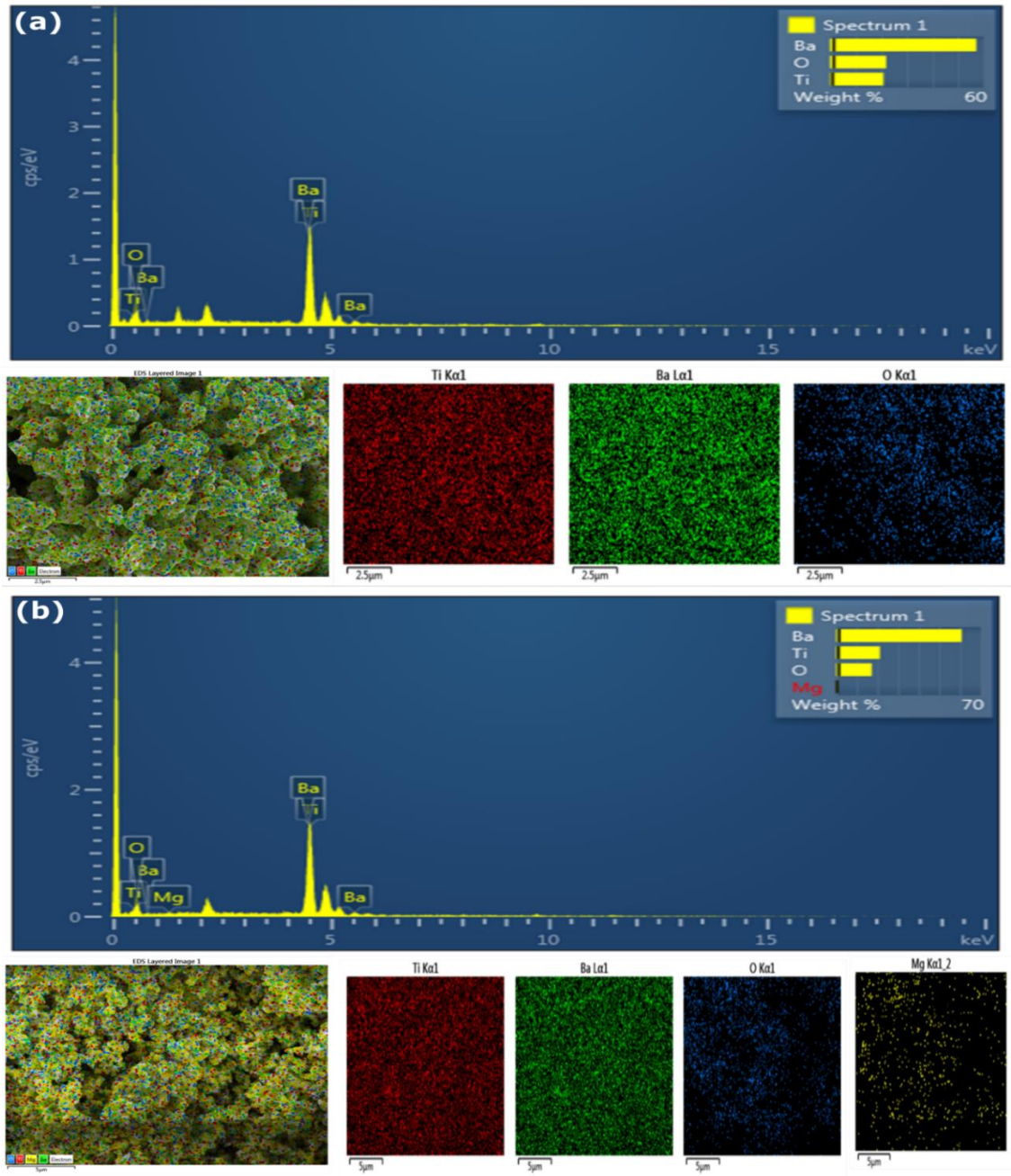

Fig 3: EDX spectra and mapping of $Ba_{1-x}Mg_xTiO_3$ (x = 0.00, and 0.20).

Conclusion

In this paper we synthesized Pure and Mg doped barium titanate ceramics by sol-gel autonomation method. ($Ba_{1-x}Mg_xTiO_3$ (x = 0.00, and 0.20). The X-ray diffraction patterns confirms the formation of perovskite structure with a single phase, a powerful absorption peak is indicated at 495cm^{-1} by the pure barium titanate while 497cm^{-1} and 499cm^{-1} absorbance peaks are observed by the doped composites of x = 0.10 and 0.015 respectively by the Fourier Transform Infrared spectroscopy, micrographs in the Field Emission Scanning Electron Microscopy confirm the presence of polycrystalline microstructures with definite degree of porosity in good agreement with XRD findings, the particles also follow a normal distribution, Energy dispersive Spectroscopy validate the emergence of Ba, Ti, and O and some Mg impurities of insignificant amount.

Acknowledgement

The authors are grateful to the Materials Research Centre, Malaviya National Institute of technology, Jaipur, India, for FE-SEM /EDX spectroscopy, XRD, FTIR characterizations.

Conflict of interest

The author declares no conflict of interest

Reference

[1] N. J. Joshi, V. Shrinet, and A. Pratap, "Influence of Metal Doping on Electrical Properties of Nano Barium Titanate," vol. 2, no. 1, pp. 1–6, 2015, doi: 10.1166/adel.2015.1033.

[2] L. Chen, Q. Fu, Z. Jiang, J. Xing, Y. Gu, and F. Zhang, "Journal of the European Ceramic Society Cathodoluminescence evaluation of the degradation of Mg , Ca and Dy Co-doped BaTiO 3 Ceramics," *J. Eur. Ceram. Soc.*, no. March, 2021, doi: 10.1016/j.jeurceramsoc.2021.08.017.

[3] K. M. Batoo, R. Verma, A. Chauhan, R. Kumar, M. Hadi, and O. M. Aldossary, "Journal of Alloys and Compounds," vol. 883, 2021.

[4] V. Paunovic, V. V Mitic, and L. Kocic, "Dielectric characteristics of donor-acceptor modi fi ed BaTiO 3 ceramics," 2016, doi: 10.1016/j.ceramint.2016.04.087.

[5] W. Cai, C. L. Fu, J. C. Gao, and C. X. Zhao, "Dielectric properties and microstructure of Mg doped barium titanate ceramics," vol. 110, no. 3, pp. 181–185, 2011, doi: 10.1179/174367611OY.0000000019.

[6] H. Search, C. Journals, A. Contact, M. Iopscience, and I. P. Address, "Effects of Oxygen Vacancies on Relaxation Behavior of Mg-Doped BaTiO3 Effects of Oxygen Vacancies on Relaxation Behavior of Mg-Doped BaTiO 3," vol. 7797, pp. 8–12, doi: 10.1143/JJAP.45.7797.

[7] K. Park, C. Kim, Y. Yoon, S. Song, Y. Kim, and K. Hur, "Doping behaviors of dysprosium , yttrium and holmium in BaTiO 3 ceramics," vol. 29, pp. 1735–1741, 2009, doi: 10.1016/j.jeurceramsoc.2008.10.021.

[8] Y. Wang, L. Li, J. Qi, and Z. Gui, "Ferroelectric characteristics of ytterbium-doped barium zirconium titanate ceramics," vol. 28, pp. 657–661, 2002.

[9] A. Alshoaibi, M. B. Kanoun, B. U. Haq, S. Alfaify, and S. Goumri-said, "Insights into the Impact of Yttrium Doping at the Ba and Ti Sites of BaTiO 3 on the Electronic Structures and Optical Properties : A First- Principles Study," 2020, doi: 10.1021/acsomega.0c01638.

[10] X. Wang, "Preparation , synthesis and application of Sol-gel method University Tutor : Pr . Olivia GIANI Internship Tutor : Mme . WANG Zhen," no. October, 2020.

[11] D. Bokov *et al.*, "Nanomaterial by Sol-Gel Method : Synthesis and Application," vol. 2021, 2021.

[12] A. I. Journal, "Study the Structural and Dielectric Properties of Rare-Earth La Doped (Ba 1-x La x) Study the Structural and Dielectric Properties of Rare-Earth La Doped (Ba 1-x La x)," vol. 4587, no. December, 2015, doi: 10.1080/10584587.2015.1105067.

[13] A. G. A. Zubeda and B. I. Haider, "Synthesis and Characterization of Nano Sized Pure and Doped Barium Titanate Powders Prepared by Sol-Gel Emulsion Technique Under the Supervision of," 2013.

[14] C. Hai *et al.*, "Surfactant-assisted synthesis of mono-dispersed cubic BaTiO 3 nanoparticles," *Mater. Res. Bull.*, vol. 57, pp. 103–109, 2014, doi: 10.1016/j.materresbull.2014.05.036.

[15] M. Ganguly, S. K. Rout, H. Y. Park, C. W. Ahn, and I. W. Kim, "Structural , dielectric and optical characterization of cerium doped barium titanate," pp. 1–12, 2013.

[16] A. Kumari and B. D. Ghosh, "La doped barium titanate / polyimide nanocomposites : A study of the effect of La doping and investigation on thermal , mechanical and high dielectric properties," vol. 46826, pp. 1–12, 2018, doi: 10.1002/app.46826.

[17] M. K. Hossain *et al.*, "A review on recent applications and future prospects of rare earth oxides in corrosion and

thermal barrier coatings , catalysts , tribological , and environmental sectors," *Ceram. Int.*, vol. 48, no. 22, pp. 32588–32612, 2022, doi: 10.1016/j.ceramint.2022.07.220.

Cite this article

Lariski F.M. and Abdulsalam H. (2023). Structural Analysis of Pure and Magnesium Doped Barium Titanate Ceramic. FUAM Journal of Pure and Applied Science, **3**(**2**):103-109